Growth of Pulmonary Microvasculature in Ventilated Preterm Infants

Monique E. De Paepe, Quanfu Mao, Jessica Powell, Sam E. Rubin, Philip DeKoninck, Naomi Appel, Meredith Dixon, and Füsun Gundogan

Department of Pathology, Women and Infants Hospital; and Department of Pathology, Brown Medical School, Providence, Rhode Island

Rationale: **Density-based morphometric studies have demonstrated decreased capillary density in infants with bronchopulmonary dysplasia (BPD) and in BPD-like animal models, leading to the prevailing view that microvascular development is disrupted in BPD.**
Objective: **To perform a comprehensive analysis of the early and late effects of ventilation on pulmonary microvascular growth in preterm infants.**
Methods: **Postmortem lung samples were collected from ventilated preterm infants who died between 23 and 29 wk ("short-term ventilated") or between 36 and 39 wk ("long-term ventilated") corrected postmenstrual age. Results were compared with age-matched infants or stillborn infants ("early" and "late" control subjects). Microvascular growth was studied by anti–platelet endothelial cell adhesion molecule (PECAM)-1 immunohistochemistry, quantitative stereology, analysis of endothelial cell proliferation, and Western blot analysis of pulmonary PECAM-1 protein levels.**
Measurements: **Measurements were made of capillary density, volume of air-exchanging parenchyma, volume of microvascular endothelial cells, Ki67 labeling index of endothelial cells, and PECAM-1/actin protein levels.**
Main Results: **Lungs of long-term ventilated infants showed a significant (more than twofold) increase in volume of air-exchanging parenchyma and a 60% increase in total pulmonary microvascular endothelial volume compared with late control subjects, associated with 60% higher pulmonary PECAM-1 protein levels. The marked expansion of the pulmonary microvasculature in ventilated lungs was, at least partly, attributable to brisk endothelial cell proliferation. The microvasculature of ventilated lungs appeared immature, retaining a saccular architectural pattern.**
Conclusions: **The pulmonary microvasculature of ventilated preterm infants displayed marked angiogenesis, nearly proportionate to the growth of the air-exchanging lung parenchyma. These results challenge the paradigm of microvascular growth arrest as a major pathogenic factor in BPD.**

Keywords: bronchopulmonary dysplasia; chronic lung disease of prematurity; neonatal lung disease

Despite major advances in perinatal medicine, including the introduction of surfactant therapy, antenatal glucocorticoids, and new ventilator strategies, preterm newborns treated with ventilation and supplemental oxygen frequently develop bronchopulmonary dysplasia (BPD), a chronic lung disease of newborn infants associated with significant mortality and morbidity (1). BPD in the postsurfactant era is seen primarily in very low birth weight infants and affects 30% of infants born at 24 to 28 wk, many of whom will require long-term ventilation and/or supplemental oxygen (2, 3).

The dominant pathologic finding at autopsy in postsurfactant BPD is an arrest in alveolar development, resulting in lungs with large and simplified airspaces showing varying degrees of interstitial fibrosis (2, 4–8). Impairment of alveolar formation in BPD leads to long-term global reduction in alveolar number and gas-exchange surface area (6, 7). The histologic pattern of alveolar hypoplasia in BPD is believed to be caused by ventilation-induced disruption of the normal sequence of lung development in newborns born during the late canalicular stage (23–27 wk of gestation). The mechanism of arrested alveolar development in BPD is unknown, although oxidant injury/hyperoxia, mechanical ventilation, proinflammatory factors, glucocorticoids, bombesin-like peptides, and poor nutrition all have been implicated (1, 2, 9).

Studies have emphasized abnormalities of the pulmonary microvasculature in infants with BPD (8, 10) or in BPD-like animal models such as chronically ventilated premature baboons (11, 12). Because proper formation of the pulmonary microvasculature is believed to be required for normal alveolar development (13–16), ventilation-induced disruption of microvascular development in premature lungs has been implicated in the arrest of alveolar development that is characteristic of BPD, culminating in the "vascular hypothesis" of BPD (17).

Previous studies describing disrupted microvascular development in the lungs of infants with BPD or in BPD-like animal models were based primarily on density-based morphometric techniques that quantified the area of endothelial cells (identified immunohistochemically with the endothelial marker platelet endothelial cell adhesion molecule [PECAM]-1) relative to the total parenchymal area. In humans as well as in premature baboons, the microvascular/capillary density, so defined, was found to be significantly lower in BPD than in age-matched control subjects (10–12). However, interpretation of data derived from density-based morphometric techniques is problematic. The decreased ratio of endothelial area to parenchymal area reported in BPD-related studies uniformly has been attributed to reduction of the endothelial area. However, a decreased endothelial-to-parenchymal ratio may alternatively be due to increased non-endothelial parenchymal area, or to a combination of both. This distinction is particularly relevant in the context of BPD, a lung disease typically associated with varying degrees of parenchymal expansion by fibrosis and edema.

The methodologic problems inherent in density-based morphometry are circumvented by application of quantitative stereologic techniques. Stereologic volumetry is the method of choice for selective determination of the volume of an identifiable cell population, such as microvascular endothelial cells, within a larger volume, such as the lung. In contrast to density-based morphometry, quantitative stereology allows determination of absolute, rather than relative, quantities (18, 19). Furthermore, by using strict random-sampling procedures, stereologic approaches ensure that the data obtained are unbiased and representative of the whole organ studied.

(*Received in original form June 15, 2005; accepted in final form October 6, 2005*)

Supported in part by National Institutes of Health P20-RR18728 (M.E.D.P.).

Correspondence and requests for reprints should be addressed to Monique E. De Paepe, M.D., Women and Infants Hospital, Department of Pathology, 101 Dudley Street, Providence, RI 02905. E-mail: mdepaepe@wihri.org

Am J Respir Crit Care Med Vol 173. pp 204–211, 2006
Originally Published in Press as DOI: 10.1164/rccm.200506-927OC on October 6, 2005
Internet address: www.atsjournals.org

The aim of the present study was to perform a comprehensive analysis of the early and late effects of mechanical ventilation on microvascular development in the lungs of preterm infants, using quantitative stereologic techniques in conjunction with Western blot analysis of PECAM-1 expression and assessment of endothelial cell proliferative activity. We report that immature lungs of ventilated preterm infants show expansion, rather than disruption, of the microvascular network, attributable in part to brisk endothelial cell proliferation. These findings challenge the widely accepted paradigm that ventilation-induced disruption of microvascular development in immature lungs is a key structural change contributing to BPD/chronic lung disease in preterm infants.

METHODS

Patients

Lung samples from ventilated and control infants were obtained from the Women and Infants Hospital (Providence, RI) perinatal autopsy files between 2001 and 2004. Informed consent was obtained in compliance with institutional guidelines. Medical and autopsy records of patients were reviewed. Infants with congenital, chromosomal, or cardiac anomalies or with other conditions potentially predisposing to pulmonary anomalies (20) were excluded. In addition, cases with documented lung hypoplasia, defined as a lung-to-body weight ratio below the 10th percentile for age, were excluded. Records were reviewed for postmenstrual age (PMA) at birth, postnatal age, and corrected postmenstrual age at death (gestational age at birth plus postnatal age). In all patients, the postmortem interval (i.e., time between death and autopsy for newborns and time between delivery and autopsy for stillborns) was recorded.

To study the early and late effects of ventilation on the immature pulmonary microvasculature, patients were divided in four groups: "short-term ventilated," "long-term ventilated," "early control," and "late control." The short-term ventilated group was composed of very preterm infants (23–29 wk PMA at the time of death), who had lived for at least 5 d and had been ventilation dependent throughout life. The long-term ventilated group consisted of near-term or term infants (36–39 wk PMA at death) who had lived for prolonged periods of time (at least 6 wk), and had been ventilated for most of their life (at least 75% of their total life span). The pulmonary vasculature of short- and long-term ventilated infants was compared with that of early control and late control patients, respectively. Control patients consisted of age-matched nonmacerated fetuses whose intrauterine demise immediately preceded delivery or live born infants who lived for less than 24 h. Control subjects were age-matched with the ventilated infants with respect to the time of death: early control infants or fetuses had died between 23 and 29 wk PMA, late control subjects between 36 and 39 wk PMA. Alternative control patients for the long-term ventilated group, representing nonventilated infants born between 23 and 29 wk who died between 36 and 39 wk PMA, were not available for study.

Lung Processing

Autopsies were performed at the Women and Infants Hospital according to standard methods. After thorough *in situ* examination, the lungs were dissected and weighed. Biopsies taken from the right upper lobe were treated with RNA*later* (Ambion, Inc., Austin, TX), as described previously (21). The remainder of the right lung was immersed in formalin. The left lung was inflation-fixed with formalin at a standardized pressure of 20 cm H_2O. After overnight fixation, the volume of the left lung was measured by volume displacement (22).

A design-based strategy was used for random sampling of the fixed left lung (18, 19, 23). The lung was serially sectioned into 5-mm-thick slices along a parasagittal plane. Tissue blocks (two to four per lung) were selected by systematic random sampling, embedded in paraffin, serially sectioned at a thickness of 5 μm, and stained with hematoxylin and eosin.

Immunohistochemical Staining

Sections of left lung were processed for avidin–biotin–immunoperoxidase staining, using anti–PECAM-1 antibody (goat polyclonal anti–PECAM-1 [M-20], sc-1506; Santa Cruz Biotechnology, Santa Cruz, CA). Binding was detected with 3,3′-diaminobenzidine tetrachloride. Sections were lightly counterstained with Mayer's hematoxylin, cleared, and mounted. Controls for specificity consisted of omission of the primary antibody.

Stereologic Morphometric Analysis of Pulmonary Microvasculature

Morphometry of the PECAM-1–immunoreactive pulmonary microvascular compartment was performed by standard stereologic volumetric techniques (18, 19, 23, 24). Consecutive steps in the structural hierarchy involved point-counting methods using a computerized image analysis system (Olympus BX-40 microscope; Olympus America, Melville, NY) interfaced via a charge-coupled device video camera (KP-161; Hitachi, Norcross, GA) to a Power Macintosh (Apple Computer Corp., Cupertino, CA) equipped with image analysis software (NIH Image; National Institutes of Health, Bethesda, MD). We used a systematic sampling method to evaluate random, nonoverlapping calibrated fields (18) for each variable described below. At least 20 microscope fields were examined for each type of measurement, as this number was found to yield reproducible results with little variance in pilot studies (a coefficient of error < 0.02 for all morphometric parameters studied). Data derived from measurements of the left lung were extrapolated to both lungs, based on the wet weight of right and left lungs. Tissue sections were examined without knowledge of the patient from whom the tissue was derived.

The critical dataset and hierarchic equations, obtained by examining the lungs at increasing levels of magnification, were similar to those described elsewhere for determination of alveolar epithelial type II cell volume (24). The parenchymal areal density (A_A[pa/lu]) was estimated by dividing the number of points falling on parenchyma (lung excluding large-sized bronchi and blood vessels) by the number of points falling on the entire lung (magnification, ×10). The parenchymal volume (V[pa]) was calculated by multiplying the total lung volume (V[lu]), by A_A(pa/lu). The areal density of air-exchanging parenchyma (A_A[ae/pa]) was estimated using random fields of peripheral lung parenchyma and dividing the number of points falling on air-exchanging parenchyma (peripheral lung parenchyma excluding airspace) by the number of points falling on the entire field (tissue and airspace; magnification, ×100). The total volume of air-exchanging parenchyma (V[ae]) was calculated by multiplying the areal density by V(pa).

The areal density of the PECAM-1–immunoreactive microvascular endothelial compartment (A_A[end/ae]) was evaluated semiautomatically, because the immunohistochemical anti–PECAM-1 staining of endothelial cells produced a higher optical density than that of the background. For each section, the light intensity was standardized by threshold calibration, using PECAM-1–negative interstitial tissue as standard. A_A(end/ae), representing the PECAM-1–immunoreactive (endothelial) area per unit area of air-exchanging parenchyma, was determined by dividing the points falling on PECAM-1–immunoreactive cells by the points falling on air-exchanging parenchyma (magnification, ×200). To avoid inclusion of endothelial cells from large-sized vascular structures in the measurements, morphometric analysis was limited to air-exchanging parenchyma. The total microvascular endothelial cell volume (V[end]) was calculated by multiplying the areal density by V(ae).

Analysis of Proliferative Activity

The spatiotemporal patterns of cell proliferation in control and ventilated lungs were studied by immunohistochemistry using anti–Ki-67 antibody (DakoCytomation, Glostrup, Denmark) in the avidin-biotin immunoperoxidase system. The proliferative rate of endothelial cells within the air-exchanging parenchyma was determined by double-immunofluorescence staining for Ki-67 and PECAM-1. Tissue sections were incubated sequentially with monoclonal anti–Ki-67, fluorescein-labeled anti-mouse IgG (Vector Laboratories, Burlingame, CA), polyclonal goat anti–PECAM-1, and Cy3-labeled anti-goat IgG (Jackson ImmunoResearch Laboratories, West Grove, PA). Controls consisted of omission of one or both primary antibodies, which abolished the respective immunoreactivities. The number of Ki-67–positive endothelial cells per high-power field was determined by manual counting. At least 25 randomly selected microscope fields were counted per lung. Analysis was limited to the distal air-exchanging parenchyma and excluded endothelium from larger sized vascular structures.

Western Blot Analysis

Pulmonary PECAM-1 protein levels were evaluated by Western blot analysis of whole lung lysates, as described in detail elsewhere (21, 25), using goat anti–PECAM-1 (Santa Cruz Biotechnology) antibody.

Data Analysis

Values are expressed as means ± SD or, where appropriate, as means ± SEM. The significance of differences between ventilated and control groups was determined by unpaired Student *t* test or by nonparametric Mann-Whitney U test where indicated. The significance level was set at $p < 0.05$. StatView software was used for all statistical work.

RESULTS

Patients

The age distribution, relevant clinical data, and autopsy findings in control and ventilated infants are summarized in Table 1. The mean postmortem interval was 15.2 ± 4.3 h for ventilated infants (range, 1–47 h) and 18.3 ± 4.2 h for control fetuses and infants (range, 6–45 h, not significantly different from the mean postmortem interval of ventilated infants).

Lung Histology

Lungs of early control infants (23–29 wk gestational age) showed large smooth-walled cylindrical acinar structures separated by relatively wide septa, characteristic of the canalicular stage of lung development. In addition to these primitive acini, focal incipient septation of the acinar units by vascularized ridges ("secondary crests") was noted, heralding the onset of the saccular stage of development (Figure 1A). A well-developed capillary network was present within the peripheral mesenchyme, "canalizing" the potential airspaces (Figure 1A). Lungs of age-matched, short-term, ventilated infants showed varying degrees of septal widening and hypercellularity, often associated with focal pulmonary hemorrhage and interstitial emphysema (Figure 1B).

Late control lungs (36–39 wk gestational age) showed a predominantly saccular architecture, with focal evidence of transition to the alveolar stage (Figure 1C). Lungs of age-matched, long-term, ventilated infants showed simplified peripheral lung architecture with lack of secondary crest formation and alveolarization (Figure 1D). Varying degrees of septal thickening with increased interstitial cellularity and fibrosis were noted. In addition, focal cuboidal epithelial cells, focal intraalveolar macrophage aggregates, and hemorrhage were noted. At all ages, the morphologic appearance of the lungs was similar in stillborn fetuses and in newborns who had lived for less than 24 h, justifying the combination of these two types of control subjects into one group for this study.

PECAM-1 Immunohistochemistry

PECAM-1 immunostaining of early control lungs at 23 to 29 wk (late canalicular/saccular stage) revealed a double capillary network within the septa, frequently localized immediately beneath the alveolar epithelial lining (Figure 2A). Lungs of short-term ventilated infants of the same age displayed abundant microvascular structures within the septa, both subepithelially and centrally (Figure 2B). Although the size of the septal microvessels varied greatly, they were mostly small caliber and were disarrayed within the interstitium. PECAM-1 immunostaining appeared less intense in early ventilated lungs compared with control subjects.

Late control lungs (36–39 wk) showed focal or diffuse transition of the capillary network within the alveolar walls to a single structure (Figure 2C). The capillary network showed frequent branching, with extension of capillary branches into secondary crests and alveolar septa. Long-term ventilated lungs showed abundant microvascular structures within the widened interstitium (Figure 2D). The septal capillaries in late ventilated lungs varied in size, ranging from short nubbins to longer segments spanning the length of the airspace, and were distributed evenly within the septal mesenchyme. Capillaries could often be seen immediately subjacent to the epithelium and displayed less branching than in late control subjects (Figure 2D). In contrast to short-term ventilated lungs, PECAM-1 staining in long-term ventilated lungs appeared to be similar or more intense than in control subjects. Omission of primary antibody or incubation with nonimmune serum abolished all staining (data not shown).

Stereologic Morphometric Analysis of the Pulmonary Microvasculature

A standard cascade approach was used to quantify the microvascular compartment in control and ventilated lungs by stereologic volumetry (18, 19, 23, 24). As shown in Table 2, the V(lu) and V(pa) (excluding large-sized hilar vascular and bronchial structures) of short- and long-term ventilated lungs were significantly larger than those of age-matched control subjects ($p < 0.01$). Similarly, the V(ae) was significantly larger in ventilated infants, consistent with ventilation-induced expansion of the distal lung parenchyma.

The PECAM-1–immunoreactive (endothelial) area relative to air-exchanging parenchymal area, A_A(end/ae), tended to be smaller in ventilated lungs compared with control subjects (17.4 vs. 19.5% in the early group and 18.9 vs. 21.6% in the late group; differences not significant). However, the total microvascular endothelial volume, V(end), the product of V(ae) and A_A(end/ae), was 30% larger in short-term ventilated lungs than in early control subjects (3.93 ± 0.98 vs. 2.91 ± 1.36 ml; not significant)

TABLE 1. CLINICAL DATA

	Early (*23–29 wk*)		Late (*36–39 wk*)	
	Control (*n = 10*)	Ventilated (*n = 7*)	Control (*n = 7*)	Ventilated (*n = 6*)
Age at birth, wk*	25.7 ± 2.4	24.7 ± 1.9	37.6 ± 1.0	27.5 ± 3.8
Postnatal age, d	< 1	9.6 ± 5.2	< 1	62.7 ± 23.0
Corrected age at death, wk*	25.9 ± 2.5	25.9 ± 2.3	37.6 ± 1.0	37.5 ± 1.2
Sex	5 M/5 F	5 M/2 F	4 M/3 F	4 M/2 F
Body weight at autopsy, g	711 ± 196	749 ± 274	2,824 ± 431	3,605 ± 1,446
Clinical/autopsy diagnosis	PROM (3); abruptio (2); sepsis ± chorioamnionitis (4); COD undetermined (1)	Early BPD with complications of prematurity (3); early BPD with sepsis (4)	Sepsis (2); abruptio (1); placental insufficiency (1); COD undetermined (3)	BPD (1); BPD with sepsis (2); BPD with NEC (1); BPD with viral infection (2)

Definition of abbreviations: BPD = bronchopulmonary dysplasia; COD = cause of death; F = female; M = male; NEC = necrotizing enterocolitis; PROM = premature rupture of membranes.

Values represent means ± SD of (n) patients.

* Age and corrected age reflect postmenstrual age.

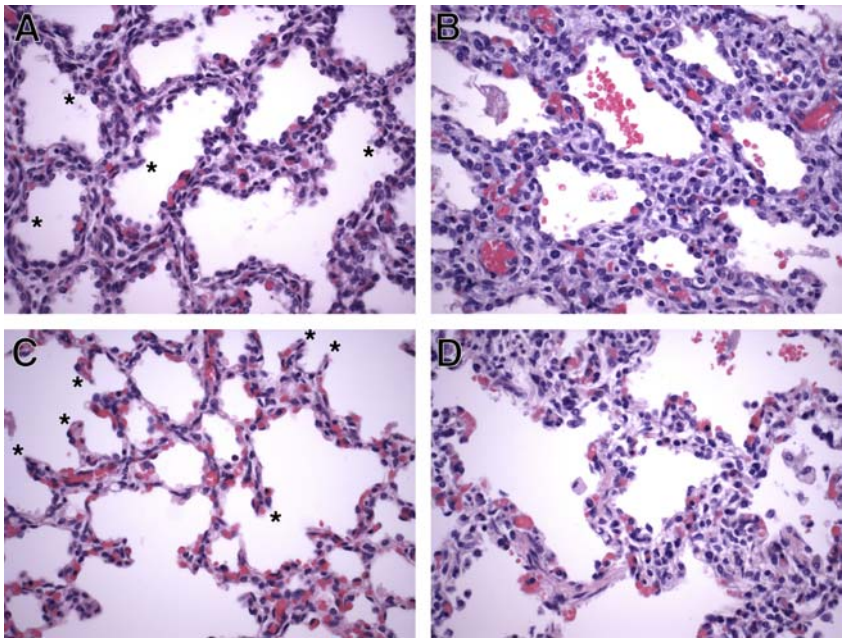

Figure 1. Lung histology. (*A*) Early control lung showing large-sized, simple airspaces, relatively wide septa, and focal early secondary crest formation (*asterisks*), characteristic of late canalicular/early saccular stage of lung development (infant born at 24 wk gestation, lived for 2 h). (*B*) Short-term ventilated lung showing widening and increased cellularity of the septa, as well as focal hemorrhages within the air spaces (infant born at 23 wk, lived for 7 d, ventilated). (*C*) Late control lung showing complex gas-exchanging parenchyma with abundant secondary crests (*asterisks*) and thin alveolar septa, consistent with late saccular/early alveolar stage of lung development (stillborn at 38 wk). (*D*) Long-term ventilated lung showing simple, large-sized air spaces with hypercellular and thickened septa (infant born at 27 wk, lived for 12 wk, ventilated). Hematoxylin–eosin staining; original magnification, ×400.

and was significantly (60%) larger in long-term ventilated lungs than in age-matched control subjects (12.16 ± 3.97 vs. 7.50 ± 3.34 ml; $p < 0.05$).

Analysis of Proliferative Activity

To determine whether the observed expansion of the microvascular endothelium was attributable to cell proliferation, we first studied the spatiotemporal patterns of proliferative activity in peripheral air-exchanging parenchyma of control and ventilated infants by immunohistochemical analysis of the proliferation marker Ki-67. In early control lungs, between 23 and 29 wk gestational age (late canalicular/saccular stage), proliferative activity was evenly distributed over alveolar epithelium and septal interstitium (Figure 3A). In short-term ventilated infants, the pulmonary proliferative activity was threefold higher compared with control subjects ($p < 0.01$), associated with a shift toward predominantly interstitial localization (Figure 3B). The proliferative rates of late control lungs between 36 and 39 wk (transition from saccular to alveolar stage) were slightly lower than those seen in preterm lungs (Figure 3C), with the majority of proliferating cells localized to the alveolar epithelial lining. Lungs of age-matched, long-term, ventilated infants showed a significant twofold increase in cellular proliferation, predominantly within the interstitium (Figure 3D). Omission of Ki-67 antibody abolished all immunoreactivity, confirming the specificity of the staining reaction (not shown). Figure 3E summarizes the proliferative indices in the various groups.

To determine the specific proliferative activity of microvascular endothelium, we performed double immunofluorescence

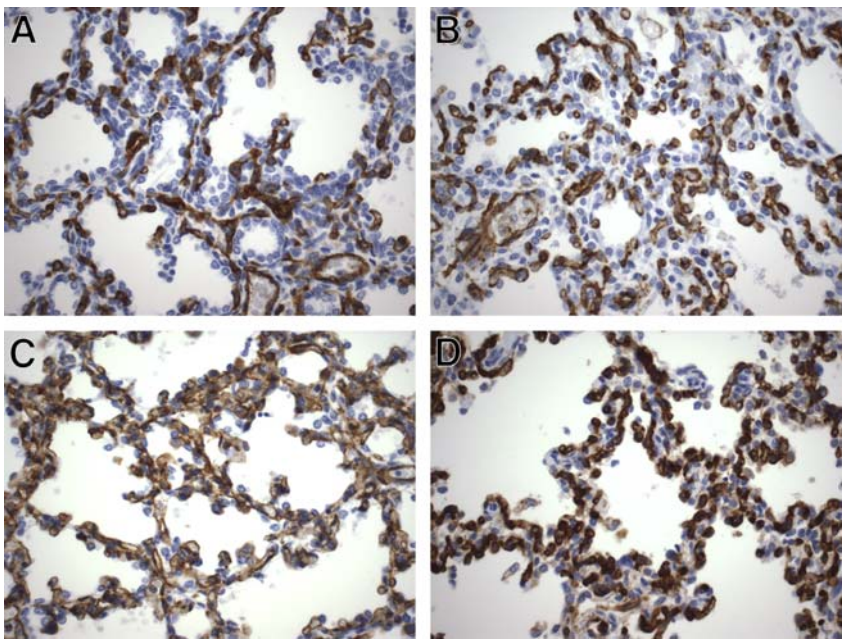

Figure 2. PECAM-1 immunohistochemistry. (*A*) Early control lung showing abundant capillary structures within the septa, often arranged in a double subepithelial capillary network (infant born at 24.5 wk gestation, lived for minutes). (*B*) Short-term ventilated lung showing abundant capillary structures of varying sizes randomly scattered within the widened septa (infant born at 23.5 wk, lived for 6 d, ventilated). (*C*) Late control lung showing a complex capillary pattern, characterized by a double or focally single capillary network with numerous outsproutings toward secondary crests (infant born at 36 wk, lived for 3 d). (*D*) Long-term ventilated lung showing abundant, intensely immunoreactive capillary structures within the thickened septa. The capillaries are prominently subepithelial, mostly arranged in a dual parallel pattern, and show few branching points (infant born at 26 wk, lived for 12 wk, ventilated, clinical diagnosis of BPD). PECAM-1 immunohistochemistry; 3,3′-diaminobenzidine tetrachloride (DAB) with hematoxylin counterstain; original magnification, ×400.

TABLE 2. STEREOLOGY DATA

	Early (*23–29 wk*)		Late (*36–39 wk*)	
	Control (*n = 10*)	Ventilated (*n = 7*)	Control (*n = 7*)	Ventilated (*n = 6*)
V(lu), ml	23.40 ± 9.07	39.98 ± 8.27*	70.84 ± 22.44	104.89 ± 33.74†
A_A(pa/lu), %	91.22 ± 1.91	88.97 ± 1.22	88.77 ± 1.77	88.33 ± 6.12
V(pa), ml	21.42 ± 8.53	35.51 ± 7.04*	62.78 ± 20.17	92.50 ± 27.98†
A_A(ae/pa), %	71.13 ± 8.68	65.18 ± 6.80	53.18 ± 9.58	75.45 ± 11.42*
V(ae), ml	14.88 ± 5.25	23.13 ± 4.94*	33.29 ± 12.81	68.48 ± 25.83*
A_A(end/ae), %	19.52 ± 5.10	17.43 ± 4.34	21.57 ± 5.86	18.92 ± 4.37
V(end), ml	2.91 ± 1.36	3.93 ± 0.98	7.50 ± 3.34	12.16 ± 3.97†

Definition of abbreviations: A_A(ae/pa) = areal density of air-exchanging parenchyma; A_A(end/ae) = areal density of PECAM-1–immunoreactive microvascular endothelial compartment; A_A(pa/lu) = parenchymal areal density; V(ae) = total volume of air-exchanging parenchyma; V(end) = total microvascular endothelial volume; V(lu) = total lung volume; V(pa) = parenchymal volume.

Values represent means ± SD of (n) lungs.

* $p < 0.01$ versus corresponding control.

† $p < 0.05$ versus corresponding control.

analysis with anti–Ki-67 and anti–PECAM-1 antibodies. In early control lungs, Ki-67–positive nuclei were evenly distributed over PECAM-1–positive endothelial cells and PECAM-1–negative epithelial and nonendothelial interstitial cells (Figure 4A). In short-term ventilated lungs, there was a dramatic increase in overall proliferative activity, associated with a brisk fourfold increase in endothelial cell proliferation (Figure 4B). The number of Ki-67–positive endothelial cells was significantly (fourfold) higher in short-term ventilated lungs compared with control subjects (Figure 4E; $p < 0.01$).

The Ki-67 labeling of late control lungs was relatively low, and evenly distributed over epithelial, endothelial, and nonendothelial cells (Figure 4C). On occasion, clustering of proliferating endothelial cells could be seen in budding secondary crests (Figure 4C, *inset*). In long-term ventilated lungs, the overall proliferative activity was more than threefold higher than in late control subjects, and continued to be present in most cell types, with predominance in adlumenal epithelial cells (Figure 4D). The proliferative activity of endothelial cells was twofold higher in long-term ventilated lungs compared with control subjects. The endothelial cell proliferation data are summarized in Figure 4E.

Analysis of Pulmonary PECAM-1 Expression

PECAM-1 protein levels were assayed by Western blot analysis of whole lung homogenates. As shown in Figure 5A, appropriately sized PECAM-1 protein bands were readily detected in early and late control lungs. In concordance with the quantitative stereology data, the PECAM-1 levels of long-term ventilated infants were significantly (65%) higher than those of late control subjects ($p < 0.05$). In contrast, pulmonary PECAM-1 levels in short-term ventilated infants were lower than those of early control subjects ($p < 0.05$). Results of densitometric quantitation of PECAM-1 band intensities, normalized to actin, are shown in Figure 5B.

DISCUSSION

We have determined the effects of short- and long-term ventilation on growth and development of the pulmonary microvasculature in preterm infants. Using standard computer-assisted stereologic volumetry, we determined that the pulmonary microvasculature of ventilated preterm lungs undergoes significant expansion, amounting to a 60% increased endothelial cell volume in long-term ventilated infants compared with age-matched late control subjects. The growth of the microvascular network is nearly proportionate to the increase in air-exchanging parenchyma noted in long-term ventilated infants. We further demonstrated by double-immunofluorescence studies that the dramatic growth of the pulmonary capillary network in ventilated lungs is, at least in part, attributable to a brisk proliferative response of endothelial cells that is most pronounced in the late canalicular/early saccular lungs of the short-term ventilated group.

The observation that ventilation induces proliferation of the pulmonary microvasculature conflicts with a prevailing notion that BPD is characterized by disruption of microvascular development and that pulmonary microvascular arrest may even play a role in the pathogenesis of this disorder. It is probable that the discrepancies between our findings and those reported previously in studies of human preterm infants (8, 10) and of chronically ventilated premature animal models of BPD (11, 12) may largely be ascribed to different methodologic approaches used to quantitate the pulmonary microvasculature.

In previous studies, the effects of ventilation on the pulmonary microvasculature have been estimated primarily by determination of capillary density and by Western blot analysis of pulmonary PECAM-1 levels. In the present study, we confirmed that the capillary density (ratio of PECAM-1–positive endothelial area to air-exchanging parenchymal area) tended to be smaller in ventilated lungs compared with control subjects (although the difference was not statistically significant). In fact, conventional density-based planimetric approaches, which are limited to determination of endothelial area relative to parenchymal area, suggest the vascular network may be diminished. However, the stereologic approach used in our study, by normalizing to the altered reference volume, V(ae), identified the actual marked expansion of the total vascular volume.

In addition to stereologic volumetry and analysis of endothelial cell proliferation, we also estimated vascular growth by analysis of pulmonary PECAM-1 protein levels. This approach was previously used by Bhatt and coworkers (10) who, in a group of infants with BPD comparable to our long-term ventilated group, determined significantly lower pulmonary PECAM-1 levels compared with age-matched control subjects. In contrast, we determined that, in long-term ventilated lungs, pulmonary PECAM-1 levels were significantly higher than in late control subjects, consistent with the observed expansion of the endothelial network. Although the cause of these conflicting results remains unclear, we speculate that differential protein degradation in postmortem tissues might have contributed to the discrepant results.

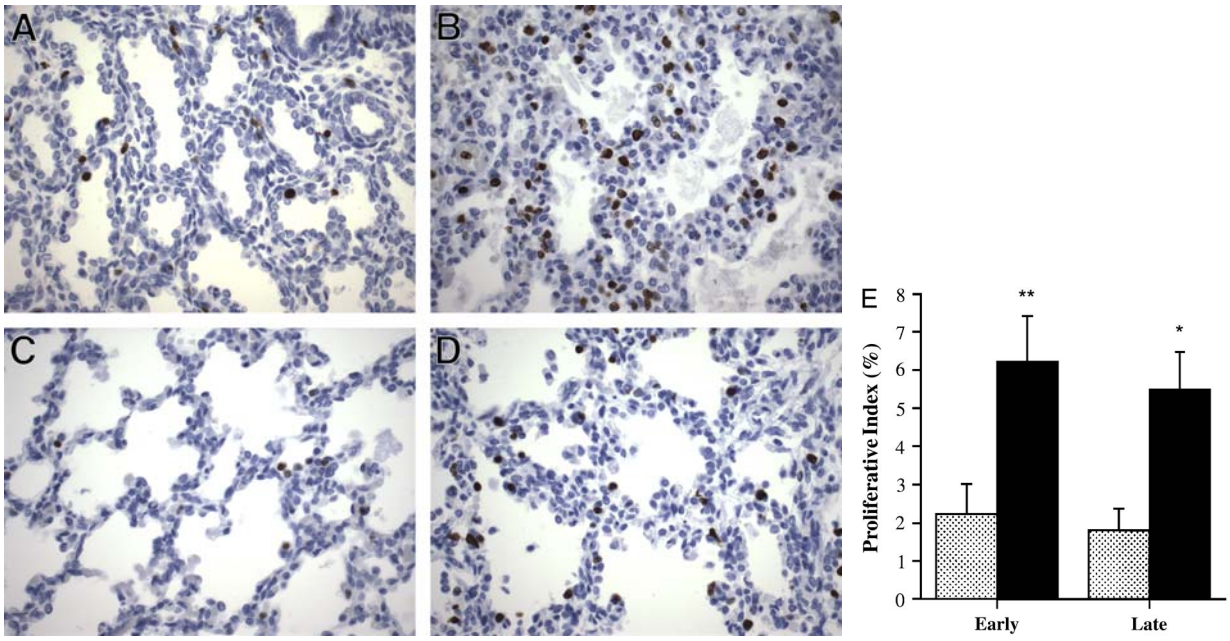

Figure 3. Ki-67 immunolabeling. (*A*) Early control lung showing scattered Ki-67–positive nuclei within the interstitium and in adlumenal (epithelial) cells (infant born at 24 wk, lived for 2 h). (*B*) Short-term ventilated lung showing markedly increased numbers of Ki-67–positive nuclei, especially within the interstitium (infant born at 23 wk, lived for 7 d, ventilated). (*C*) Late control lung showing relatively few Ki-67–positive nuclei in interstitium and epithelium (stillborn at 36 wk). (*D*) Long-term ventilated lung showing more Ki-67–positive nuclei than late control lungs, evenly distributed over interstitium and epithelium (infant born at 27 wk, lived for 11 wk, ventilated). (*E*) Lung proliferative index of early control, early (short-term) ventilated, late control, and late (long-term) ventilated infants. Values represent means ± SD of at least five patients per group. *Dotted bars*, control; *black bars*, ventilated. *p $<$ 0.05 versus control; **p $<$ 0.01 versus control. Ki-67 immunohistochemistry; DAB with hematoxylin counterstain; original magnification, ×400.

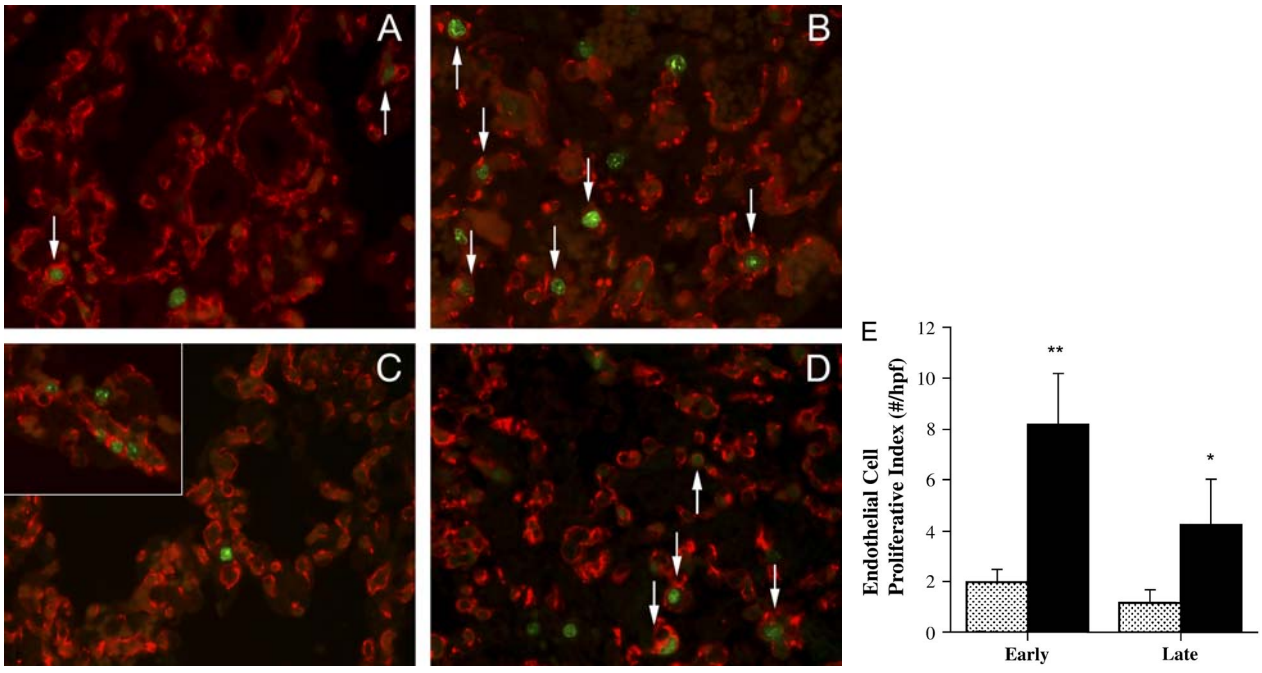

Figure 4. PECAM-1 and Ki-67 double immunofluorescence. (*A*) Early control lung showing Ki-67–positive endothelial cells (*arrows*) and nonendothelial cells (same infant as in Figure 3A). (*B*) Short-term ventilated lung showing overall increase in Ki-67 labeling, both in PECAM-positive endothelial cells (*arrows*) and in nonendothelial cells (same infant as in Figure 3B). (*C*) Late control lung showing relatively low proliferative activity. Shown is a single nonendothelial Ki-67–positive cell. *Inset*: Focal intense endothelial cell proliferation associated with secondary crest formation (same stillborn as in Figure 3C). (*D*) Long-term ventilated lung showing increased Ki-67 labeling compared with late control, both in endothelial cells (*arrows*) and in nonendothelial cells (same infant as in Figure 3D). (*E*) Endothelial cell proliferative index. Values represent means ± SD of at least five patients per group. *Dotted bars*, control; *black bars*, ventilated. *p $<$ 0.05 versus control; **p $<$ 0.01 versus control. Ki-67 (fluorescein isothiocyanate, *green*) and PECAM-1 (Cy3, *red*) double immunofluorescence; original magnification, ×400.

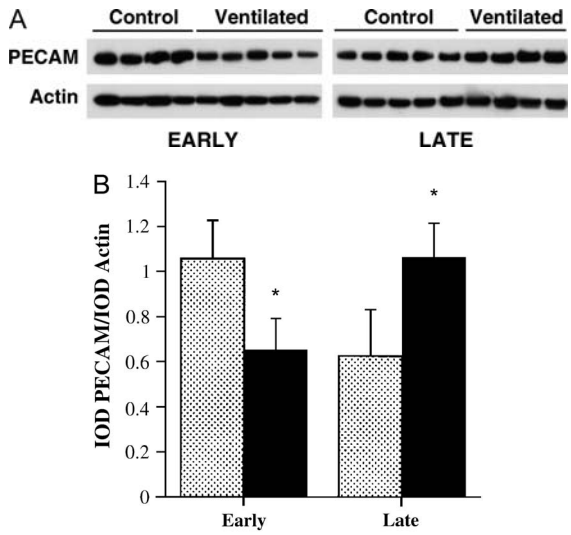

Figure 5. Western blot analysis of pulmonary PECAM-1 protein levels. (*A*) Western blot analysis of PECAM-1 protein expression in whole lung homogenates. Bands appropriately sized for PECAM-1 (~ 100 kD) were detected. Actin (42 kD) served as internal loading control. (*B*) Densitometry of PECAM-1 Western blot analysis. Values represent means ± SE. *Dotted bars*, control; *black bars*, ventilated. *$p < 0.05$ versus control. IOD = integrated optical density.

We further determined that the PECAM-1 levels in early ventilated lungs were lower than in age-matched control subjects. Similar results were reported by Maniscalco and coworkers (12) in preterm baboons ventilated for 1 to 2 wk. Our stereologic volumetry studies demonstrated a 30% increase in total microvascular endothelial volume. The apparent discrepancy between morphometry and Western blot findings can be explained, at least in part, by lower cellular PECAM-1 levels (as suggested by the immunohistochemistry findings). This discrepancy underscores the fallacy of Western blot analysis for estimation of the size of a specific cell population within a larger organ.

It needs to be emphasized that the value of Western blot analysis of PECAM-1 protein levels in whole lung homogenates as a measure of microvascular quantity is limited. First, analysis of whole lung lysates does not allow distinction between PECAM-1 protein derived from large and intermediate-sized blood vessels versus the microvessels of interest. The contribution of these various vascular compartments to total pulmonary PECAM-1 protein remains undetermined and may vary between control and ventilated lungs. Second, pulmonary PECAM-1 protein levels are determined not only by the total number of endothelial cells, but also by the PECAM-1 protein levels in the individual endothelial cells. As suggested by our immunohistochemical studies, the cellular PECAM-1 protein concentration may vary according to gestational age and ventilation status. Finally, pulmonary PECAM-1 protein levels assayed by Western blot analysis are customarily normalized to the levels of a housekeeping gene, such as actin. On the basis of the morphometric and morphologic analyses, it is evident that ventilation results in significant expansion of the interstitium, which likely results in differential increases in pulmonary actin content. Of note, the limitations of Western blot analysis delineated above are eliminated by use of stereologic volumetry.

The present study demonstrates that the postcanalicular pulmonary circulation may undergo angiogenesis when stimulated by factors associated with prolonged mechanical ventilation. In contrast to the bronchial circulation, it has been assumed that the pulmonary circulation may be relatively inert with respect to its capacity for angiogenesis (reviewed in Reference 26). However, several reports, partly supported by application of quantitative stereologic techniques, have revealed a robust angiogenic capacity in the (adult) pulmonary circulation, when properly stimulated.

The regulation of ventilation-induced angiogenesis remains to be elucidated. In a fetal baboon model of BPD, ventilation was associated with significantly decreased levels of vascular endothelial growth factor (VEGF) and its receptor Flt-1, whereas angiopoietin and its receptor were not significantly changed (12). Studies in human preterm infants have been less clear-cut, in part attributable to small sample sizes and high clinical variability. Bhatt and coworkers (10) reported decreased VEGF mRNA and decreased VEGF immunostaining in infants with BPD compared with infants without BPD. Similarly, Lassus and coworkers (27) described lower VEGF in tracheal aspirates of preterm infants with severe respiratory distress/BPD compared with control subjects. In contrast, studies by Ambalavanan and Novak (28), D'Angio and coworkers (29), and Currie and coworkers (30) found no correlation between levels of VEGF in tracheal aspirates of preterm infants and risk for development of BPD.

Our study demonstrates that ventilation induces significant expansion of the pulmonary microvasculature, nearly proportionate to the growth of the air-exchanging parenchyma. However, the capillary network in ventilated lungs was found to retain the primitive vascular pattern of canalicular/saccular lungs, characterized by a persistent dual capillary pattern and simplified, nonbranching vessels. Alignment of the septal capillaries with the alveolar epithelium is essential for effective gas exchange and crucial for viability. Although the capillaries in late-ventilated BPD lungs were frequently seen to be aligned with the alveolar lining, the paucity of branching could lower the efficiency of gas exchange in the expanding parenchyma.

In conclusion, we have shown, using quantitative stereologic and immunohistochemical double-labeling techniques, that the pulmonary microvasculature of ventilated preterm infants undergoes active angiogenesis, almost commensurate to the degree of expansion of the distal air-exchanging parenchyma. Although it needs to be acknowledged that these results represent findings in infants with severe (lethal) forms of BPD, it is likely that angiogenesis, albeit to a lesser extent, may also occur in survivors of BPD with less severe forms of this disease. In view of these findings, the potential role of quantitative alterations in the pulmonary microvascular growth in the development of BPD may need reconsideration.

Conflict of Interest Statement: None of the authors have a financial relationship with a commercial entity that has an interest in the subject of this manuscript.

Acknowledgment: The authors thank Terry Pasquariello for assistance with immunohistochemical analyses. The authors are also grateful to Francois I. Luks, M.D., Ph.D., and Lewis P. Rubin, M.D., for insightful discussions and review of the manuscript.

References

1. Jobe AH, Ikegami M. Mechanisms initiating lung injury in the preterm. *Early Hum Dev* 1998;53:81–94.
2. Jobe AH, Bancalari E. Bronchopulmonary dysplasia. *Am J Respir Crit Care Med* 2001;163:1723–1729.
3. Lemons JA, Bauer CR, Oh W, Korones SB, Papile LA, Stoll BJ, Verter J, Temprosa M, Wright LL, Ehrenkranz RA, *et al.*; NICHD Neonatal Research Network. Very low birth weight outcomes of the National Institute of Child Health and Human Development Neonatal Research Network, January 1995 through December 1996. *Pediatrics* 2001;107:E1.

4. Erickson AM, de la Monte SM, Moore GW, Hutchins GM. The progression of morphologic changes in bronchopulmonary dysplasia. *Am J Pathol* 1987;127:474–484.
5. Bonikos DS, Bensch KG, Northway WH Jr, Edwards DK. Bronchopulmonary dysplasia: the pulmonary pathologic sequel of necrotizing bronchiolitis and pulmonary fibrosis. *Hum Pathol* 1976;7:643–666.
6. Husain AN, Siddiqui NH, Stocker JT. Pathology of arrested acinar development in postsurfactant bronchopulmonary dysplasia. *Hum Pathol* 1998;29:710–717.
7. Jobe AJ. The new BPD: an arrest of lung development. *Pediatr Res* 1999;46:641–643.
8. Coalson JJ. Pathology of chronic lung disease in early infancy. In: Bland RD, Coalson JJ, editors. Chronic lung disease in early infancy. New York: Marcel Dekker; 2000. pp. 85–124.
9. Bhandari A, Bhandari V. Pathogenesis, pathology and pathophysiology of pulmonary sequelae of bronchopulmonary dysplasia in premature infants. *Front Biosci* 2003;8:e370–e380.
10. Bhatt AJ, Pryhuber GS, Huyck H, Watkins RH, Metlay LA, Maniscalco WM. Disrupted pulmonary vasculature and decreased vascular endothelial growth factor, Flt-1, and TIE-2 in human infants dying with bronchopulmonary dysplasia. *Am J Respir Crit Care Med* 2001;164: 1971–1980.
11. Coalson JJ, Winter VT, Siler-Khodr T, Yoder BA. Neonatal chronic lung disease in extremely immature baboons. *Am J Respir Crit Care Med* 1999;160:1333–1346.
12. Maniscalco WM, Watkins RH, Pryhuber GS, Bhatt A, Shea C, Huyck H. Angiogenic factors and alveolar vasculature: development and alterations by injury in very premature baboons. *Am J Physiol Lung Cell Mol Physiol* 2002;282:L811–L823.
13. Jakkula M, Le Cras TD, Gebb S, Hirth KP, Tuder RM, Voelkel NF, Abman SH. Inhibition of angiogenesis decreases alveolarization in the developing rat lung. *Am J Physiol Lung Cell Mol Physiol* 2000; 279:L600–L607.
14. Le Cras TD, Markham NE, Tuder RM, Voelkel NF, Abman SH. Treatment of newborn rats with a VEGF receptor inhibitor causes pulmonary hypertension and abnormal lung structure. *Am J Physiol Lung Cell Mol Physiol* 2002;283:L555–L562.
15. Gerber HP, Hillan KJ, Ryan AM, Kowalski J, Keller GA, Rangell L, Wright BD, Radtke F, Aguet M, Ferrara N. VEGF is required for growth and survival in neonatal mice. *Development* 1999;126:1149–1159.
16. Galambos C, Ng YS, Ali A, Noguchi A, Lovejoy S, D'Amore PA, DeMello DE. Defective pulmonary development in the absence of heparin-binding vascular endothelial growth factor isoforms. *Am J Respir Cell Mol Biol* 2002;27:194–203.
17. Abman SH. Bronchopulmonary dysplasia: "a vascular hypothesis." *Am J Respir Crit Care Med* 2001;164:1755–1756.
18. Bolender RP, Hyde DM, Dehoff RT. Lung morphometry: a new generation of tools and experiments for organ, tissue, cell, and molecular biology. *Am J Physiol* 1993;265:L521–L548.
19. Gundersen HJ, Bendtsen TF, Korbo L, Marcussen N, Moller A, Nielsen K, Nyengaard JR, Pakkenberg B, Sorensen FB, Vesterby A, *et al.* Some new, simple and efficient stereological methods and their use in pathological research and diagnosis. *APMIS* 1988;96:379–394.
20. De Paepe ME. Lung growth and development. In: Churg AM, Myers JL, Tazelaar HD, Wright JL, editors. Thurlbeck's pathology of the lung. New York: Thieme Medical Publishers; 2005. pp. 39–84.
21. De Paepe ME, Mao Q, Huang C, Zhu D, Jackson CL, Hansen K. Postmortem RNA and protein stability in perinatal human lungs. *Diagn Mol Pathol* 2002;11:170–176.
22. Scherle W. A simple method for volumetry of organs in quantitative stereology. *Mikroskopie* 1970;26:57–60.
23. Weibel ER, Cruz-Orive LM. Morphometric methods. In: Crystal RG, West JB, Weibel ER, Barnes PJ, editors. The lung: scientific foundations. Philadelphia, PA: Lippincott-Raven; 1997. pp. 333–344.
24. De Paepe ME, Johnson BD, Papadakis K, Sueishi K, Luks FI. Temporal pattern of accelerated lung growth after tracheal occlusion in the fetal rabbit. *Am J Pathol* 1998;152:179–190.
25. De Paepe ME, Mao Q, Embree-Ku M, Rubin LP, Luks FI. Fas/FasL-mediated apoptosis in perinatal murine lungs. *Am J Physiol Lung Cell Mol Physiol* 2004;287:L730–L742.
26. Mitzner W, Wagner EM. Vascular remodeling in the circulations of the lung. *J Appl Physiol* 2004;97:1999–2004.
27. Lassus P, Turanlahti M, Heikkila P, Andersson LC, Nupponen I, Sarnesto A, Andersson S. Pulmonary vascular endothelial growth factor and Flt-1 in fetuses, in acute and chronic lung disease, and in persistent pulmonary hypertension of the newborn. *Am J Respir Crit Care Med* 2001;164:1981–1987.
28. Ambalavanan N, Novak ZE. Peptide growth factors in tracheal aspirates of mechanically ventilated preterm neonates. *Pediatr Res* 2003;53:240–244.
29. D'Angio CT, Maniscalco WM, Ryan RM, Avissar NE, Basavegowda K, Sinkin RA. Vascular endothelial growth factor in pulmonary lavage fluid from premature infants: effects of age and postnatal dexamethasone. *Biol Neonate* 1999;76:266–273.
30. Currie AE, Vyas JR, MacDonald J, Field D, Kotecha S. Epidermal growth factor in the lungs of infants developing chronic lung disease. *Eur Respir J* 2001;18:796–800.